

## Research Paper

## Deep learning neural networks for spatially explicit prediction of flash flood probability



Mahdi Panahi <sup>a,b</sup>, Abolfazl Jaafari <sup>a,c</sup>, Ataollah Shirzadi <sup>d</sup>, Himan Shahabi <sup>e,f</sup>, Omid Rahmati <sup>f</sup>, Ebrahim Omidvar <sup>g</sup>, Saro Lee <sup>a,h,\*</sup>, Dieu Tien Bui <sup>i</sup>

<sup>a</sup> Geoscience Platform Research Division, Korea Institute of Geoscience and Mineral Resources (KIGAM), 124, Gwahak-ro Yuseong-gu, Daejeon 34132, Republic of Korea

<sup>b</sup> Division of Science Education, Kangwon National University, Chuncheon-si, Gangwon-do 24341, Republic of Korea

<sup>c</sup> Research Institute of Forests and Rangelands, Agricultural Research, Education, and Extension Organization (AREEO), Tehran 13185-116, Iran

<sup>d</sup> Department of Rangeland and Watershed Management, Faculty of Natural Resources, University of Kurdistan, Sanandaj 66177-15175, Iran

<sup>e</sup> Department of Geomorphology, Faculty of Natural Resources, University of Kurdistan, Sanandaj, Iran

<sup>f</sup> Kordestan Agricultural and Natural Resources Research and Education Center, Agricultural Research, Education, and Extension Organization (AREEO), Sanandaj, Iran

<sup>g</sup> Department of Rangeland and Watershed Management, Faculty of Natural Resources and Earth Sciences, University of Kashan, Kashan 87317-53153, Iran

<sup>h</sup> Department of Geophysical Exploration, Korea University of Science and Technology, 217 Gajeong-ro, Yuseong-gu, Daejeon 34113, Republic of Korea

<sup>i</sup> Institute of Research and Development, Duy Tan University, Da Nang 550000, Viet Nam

<sup>j</sup> Department of Zrebar Lake Environmental Research, Kurdistan Studies Institute, University of Kurdistan, Sanandaj, Iran

## ARTICLE INFO

## Article history:

Received 6 April 2020

Received in revised form 2 July 2020

Accepted 1 September 2020

Available online 16 December 2020

Handling Editor: E. Shaji

## Keywords:

Spatial modeling

Machine learning

Convolutional neural networks

Recurrent neural networks

GIS

Iran

## ABSTRACT

Flood probability maps are essential for a range of applications, including land use planning and developing mitigation strategies and early warning systems. This study describes the potential application of two architectures of deep learning neural networks, namely convolutional neural networks (CNN) and recurrent neural networks (RNN), for spatially explicit prediction and mapping of flash flood probability. To develop and validate the predictive models, a geospatial database that contained records for the historical flood events and geo-environmental characteristics of the Golestan Province in northern Iran was constructed. The step-wise weight assessment ratio analysis (SWARA) was employed to investigate the spatial interplay between floods and different influencing factors. The CNN and RNN models were trained using the SWARA weights and validated using the receiver operating characteristics technique. The results showed that the CNN model ( $AUC = 0.832$ ,  $RMSE = 0.144$ ) performed slightly better than the RNN model ( $AUC = 0.814$ ,  $RMSE = 0.181$ ) in predicting future floods. Further, these models demonstrated an improved prediction of floods compared to previous studies that used different models in the same study area. This study showed that the spatially explicit deep learning neural network models are successful in capturing the heterogeneity of spatial patterns of flood probability in the Golestan Province, and the resulting probability maps can be used for the development of mitigation plans in response to the future floods. The general policy implication of our study suggests that design, implementation, and verification of flood early warning systems should be directed to approximately 40% of the land area characterized by high and very susceptibility to flooding.

© 2021 China University of Geosciences (Beijing) and Peking University. Production and hosting by Elsevier B.V. This is an open access article under the CC BY-NC-ND license (<http://creativecommons.org/licenses/by-nc-nd/4.0/>).

## 1. Introduction

Floods account for an estimated 84% of all natural disaster deaths around the world (Jamali et al., 2020). Different countries experience frequent flood events, with annually US\$ 60 billion of direct economic losses (Convertino et al., 2019; Janizadeh et al., 2019) and hundreds of deaths and injuries (Haynes et al., 2017; Špitálar et al., 2020). Over the recent years, the increased changes in climate and socioeconomic status have intensified the frequency and severity of flood occurrences that in

turn have placed strong demands on managers and engineers to temporally and spatially delineate the landscapes in terms of probability to flood occurrences (Tehrany et al., 2015).

In Iran, annual floods cause hundreds of millions of dollars of damage to infrastructure and agriculture. According to the information released by the Forests, Rangelands and Watershed Management Organization of Iran, the floods caused the death of 2381 people and at least US\$ 2.3 billion in damages throughout 1950–2004. From mid-March to April 2019, large parts of Iran have been hit by widespread flash flooding that resulted in evacuating several cities and many villages in the Golestan, Mazandaran, and Khuzestan provinces. Floods killed and injured many peoples in the Fars and Lorestan provinces, collapsed at least 314 bridges,

\* Corresponding author.

E-mail addresses: [jaafari@rifr.ac.ir](mailto:jaafari@rifr.ac.ir) (A. Jaafari), [leesaro@kigam.re.kr](mailto:leesaro@kigam.re.kr) (S. Lee), [buitiendieu@duytan.edu.vn](mailto:buitiendieu@duytan.edu.vn) (D.T. Bui).

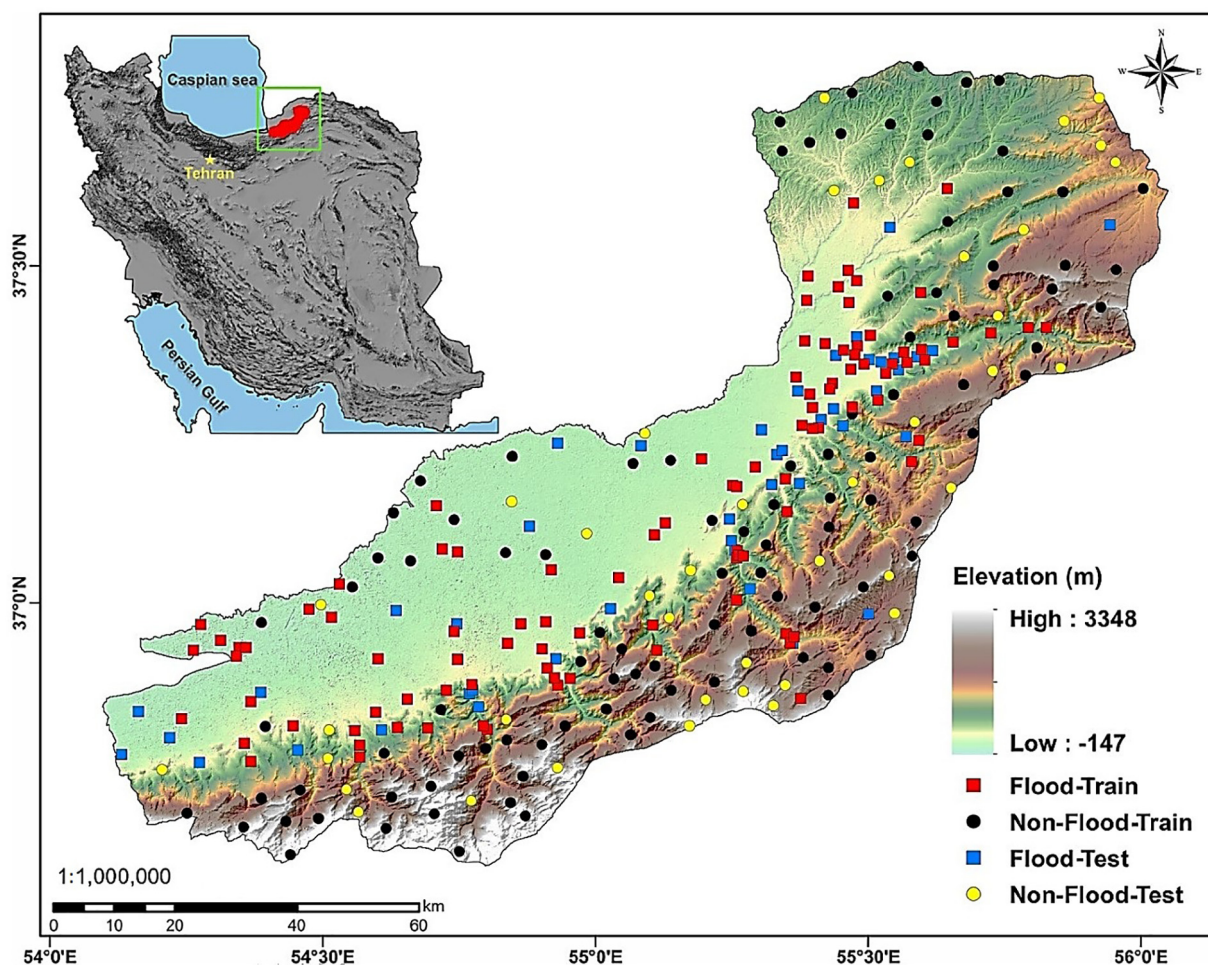


**Fig. 1.** Geographical location of the study area and flooded locations.



**Fig. 2.** Photographs of flood events in the Golestan Province of Iran (Source: ISNA and IRNA).

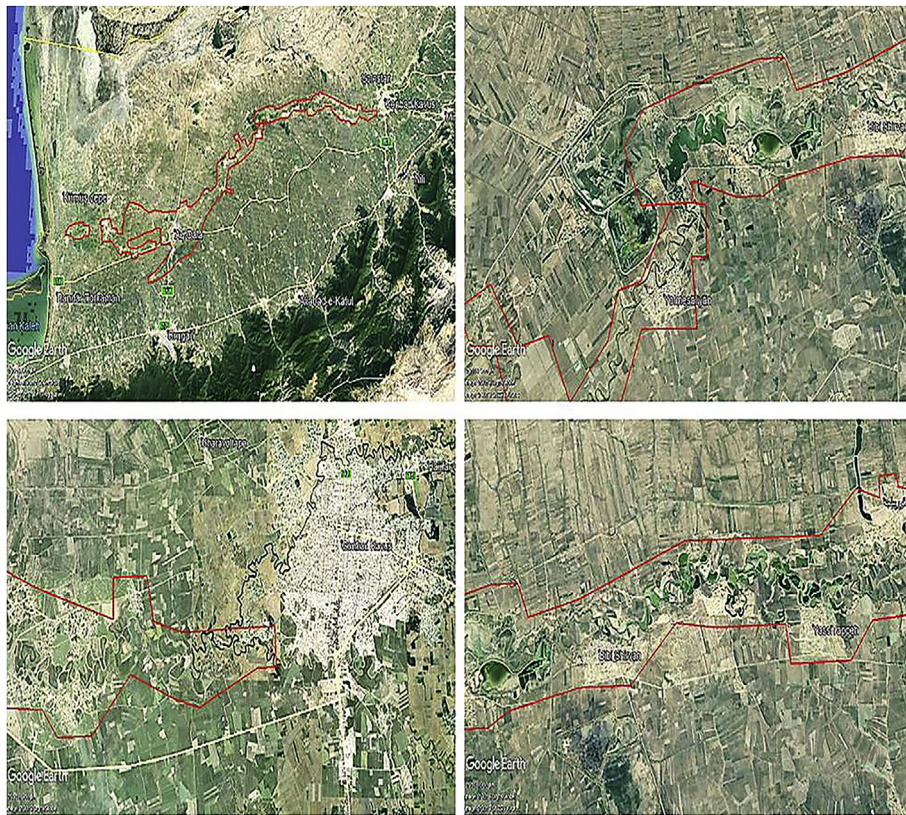


**Fig. 3.** Flood affected areas in the Golestan Province in March 2019.

destroyed 25,000 houses across the country, damaged water and agriculture infrastructure, and caused total economic losses of about US\$ 2.5 billion.

The first phase of flood management strategies is to undertake a flood hazard analysis for flood-prone areas. Flood hazard analysis identifies landscapes with high/very high floods probability to successfully guide the management plans and to allocate flood-fighting resources. To this end, powerful and reliable tools are required to enable the managers and engineers to accurately estimate the time, location, and extent of future floods (Bui et al., 2019; Choubin et al., 2019). Flood probability modeling and mapping was initially begun using straightforward and easy-to-use bivariate and multivariate statistical methods, such as frequency ratio, weights of evidence, and linear logistic regression (Khosravi et al., 2018). These methods, however, tend to simplify the complex nature of flood events and often lead to unreliable outcomes. As a replacement of these methods, machine learning methods have been suggested that have also successfully reached the primacy for the prediction of other types of natural hazards such as wildfire (Jaafari et al., 2019c), drought (Rahmati et al., 2019), earthquake (Alizadeh et al., 2018), gully erosion (Azareh et al., 2019; Nhu et al., 2020a), land/ground subsidence (Bui et al., 2018b), and landslide (Chen et al., 2019a; Jaafari et al., 2019a; Lee and Oh, 2019; Nhu et al., 2020b; Nhu et al., 2020c) as well as for other environmental problems, such as groundwater potential mapping (Pham et al., 2019; Nguyen et al., 2020a, b) and tree mortality modeling (Bayat et al., 2019).

The notable machine learning methods used for flood modeling include decision tree based classifiers (Khosravi et al., 2018; Janizadeh et al., 2019), artificial neural network (ANN) (Janizadeh et al., 2019), and support vector machine (SVM) (Tehrany et al., 2015; Choubin et al., 2019). Despite the efficacy of these methods, flood prediction at regional scales remains a challenging task due to the plurality of several unknown causative factors and their complex interactions (Sen, 2018), highlighting the need to develop and apply more advanced modeling approaches (Bui et al., 2018a; Bui et al., 2019c;). In the past few years,

various enhanced flood predictive models have emerged and proven to be highly effective for obtaining accurate estimates of future floods. Among them are neuro-fuzzy, multivariate adaptive regression splines, and extreme learning machines that benefited from metaheuristics optimization algorithms (Bui et al., 2018a; Hong et al., 2018; Ahmadlou et al., 2019; Bui et al., 2019c).

In the previous studies, flood modeling is typically formulated as a supervised learning problem, in which both inputs and outputs are labeled to obtain rules and latent relationships of data to predict the labels of unobserved data after learning. However, in this study, we present a semi-supervised modeling approach based on deep learning neural networks. These models represent a deep graph that consists of various processing layers to automatically extract knowledge from a large training dataset of historical floods, without requiring to label all datasets manually. More precisely, the development of this model allows for using both labeled and unlabeled types of data at the same time to increase the possibility that the predictive accuracy of the model is maximized. Deep learning modeling is especially interesting because this approach overcomes many of the restrictions placed on the modeling process by traditional machine learning methods (LeCun et al., 2015; Lipton et al., 2015; Sameen et al., 2019; Dao et al., 2020). However, deep learning is not a novel concept in the literature. What has changed from early ANNs is the dimension of the networks, which often represent a complex structure of connections between hundreds of layers and millions of neurons (Kraus et al., 2019). This structure provides the model with unprecedented flexibility to identify highly complex, non-linear relationships between predictor and outcome variables that has enabled deep neural networks to successfully outperform the other models derived by the traditional machine methods in a variety of tasks.

In this study, we used two types of deep learning neural networks, i.e., convolutional neural networks (CNN) and recurrent neural networks (RNN), for spatial prediction and mapping of flood probability. Despite the widespread application of these two models, they have been rarely employed for flood probability mapping over the world.

The development and application of the CNN and RNN models are underpinned by a large dataset from the Golestan Province, Iran, where floods occur frequently.

## 2. Description of the study area

The study area is located in the Golestan Province in the northeast of Iran (Fig. 1). The area lies between  $36^{\circ}27'$  to  $38^{\circ}14'$ N latitudes and  $53^{\circ}40'$  to  $56^{\circ}30'$ E longitudes and covers an area about  $12,000\text{ km}^2$  that encompasses approximately 59% of the Golestan Province. The area is characterized by a variable topography (slope =  $0\text{--}76^{\circ}$  and altitude =  $-147\text{ m}$  to  $3348\text{ m}$ ) that strongly affects the local climate. While the northern and central parts enjoy a temperate Mediterranean climate, the southern part has a mountain climate. The annual rainfall amounts vary between 250 mm and 1000 mm with an annual average of 450 mm. The lithology of the study area consists of several geologic units that belong to the Cenozoic (57.43% of the land area), Mesozoic (24.17% of the land area), Paleozoic (15.04% of the land area), Proterozoic (3.36% of the land area) geological eras.

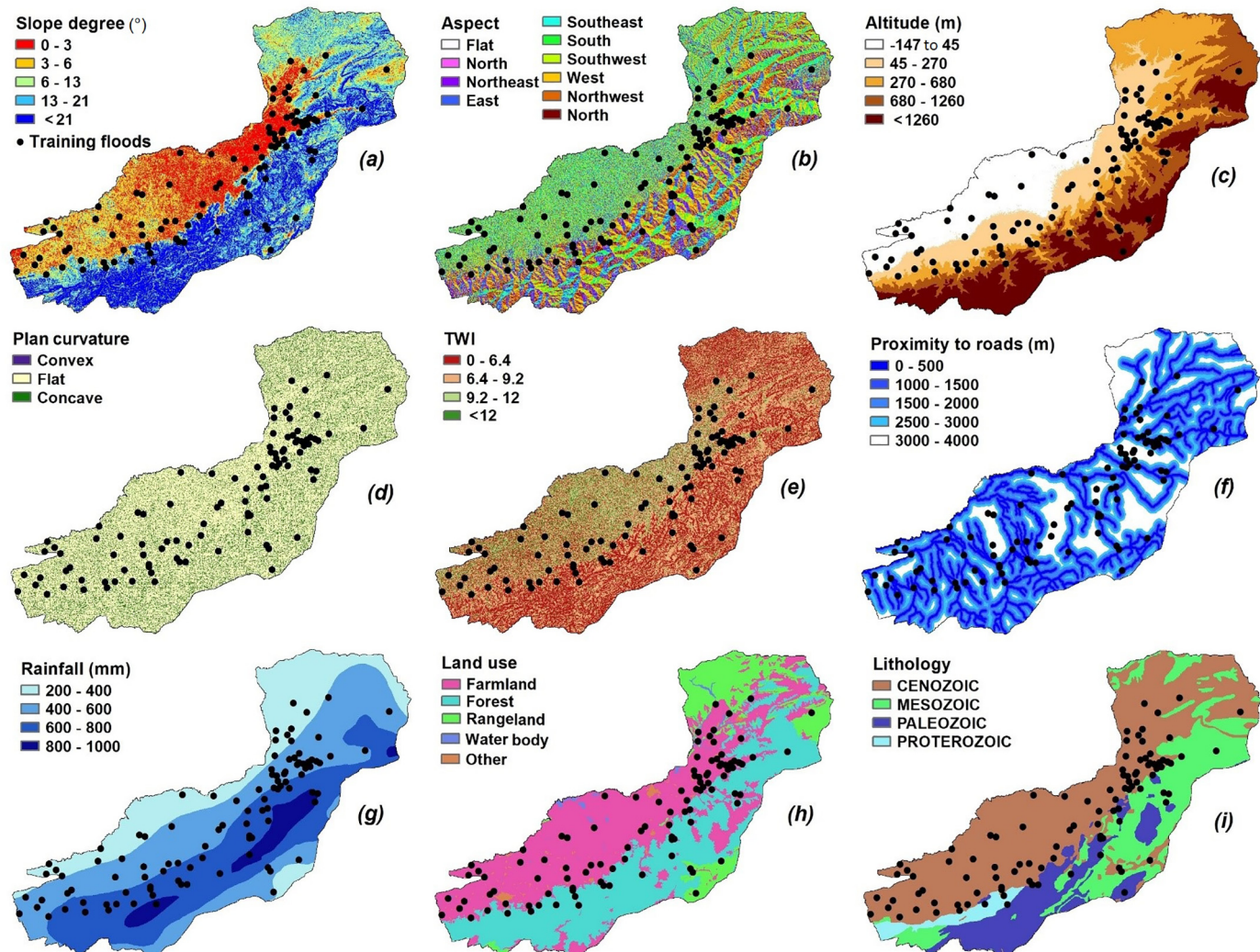
Although the area was primarily covered by forests (37.33% of the land area) and rangelands (13.58% of the land area), today a high level of agriculture development (47.20% of the land area) and urbanization with a high concentration of settlement areas, industries, and their associated infrastructure occupied this area. The study area includes the total land area of the Bandar Gaz, Kordkoy, Gorgan, Ali Abad, Ramian,

Azadshahr, Minodasht cities, and a part of the Bandar Torkaman, Gonishan Agh Ghala, Gonbad Kavous, and Kalaleh cities. The estimated human population of this area in the year 2016 was 1.37 million. Since these cities have been mostly developed along the rivers, they have experienced several floods during the last decades. The most recent devastating flood has occurred in March 2019 that left eight deaths and caused economic damage of about \$160 million (Fig. 2). During this event, in just one day in mid-March, the cumulative rainfall of 315 mm was measured that accounted for about 70% of the annual rainfall in this area (IRIMO, 2019).

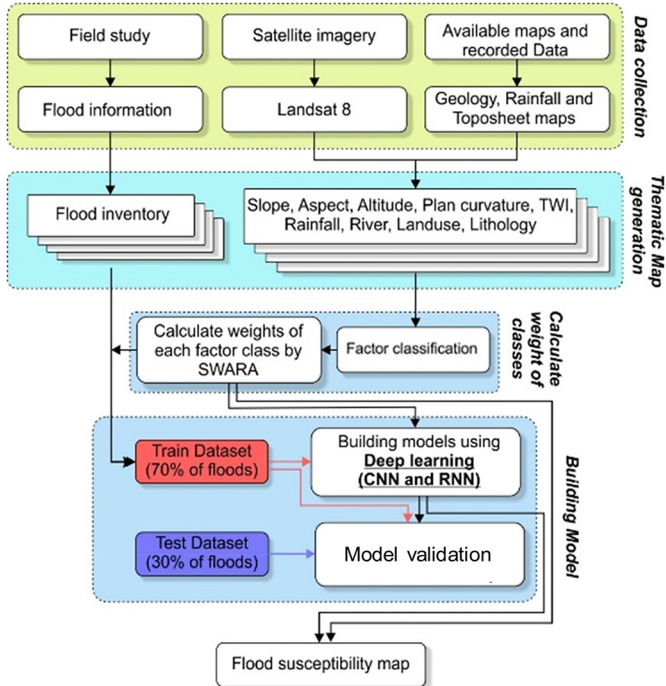
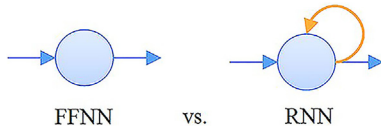
## 3. Data collection

### 3.1. Flood inventory map

Identifying and mapping the historical locations of floods is crucial for investigating the spatial interplay between flood probability and different influencing factors. Current approaches typically rely on referring to the historical archives, field surveys, and remotely sensed satellite image data. Here, we first used the historical archives of the Regional Water Organization of the Golestan Province to compile an inventory map of historical floods. We next used the Google Earth images before and after a flood event for further verification of the time and locations of the floods reported in the historical archives (Fig. 3). In total, 143 flood events from the period 2009–2019 were identified. Along



**Fig. 4.** Flood influencing factors: (a) slope, (b) aspect, (c) altitude, (d) plan curvature, (e) TWI, (f) proximity to rivers, (g) rainfall, (h) land use, and (i) lithology.

**Fig. 5.** Flowchart of the methodology.**Fig. 6.** Difference between hidden layers in FFNN and RNN.

with the flood locations, we sampled 143 locations as “unflooded location” from the areas without any evidence of flood occurrences. Flooded and unflooded locations were merged and randomly divided into groups. The first group included 70% of data (100 floods and 100 unfloods), which was used as the training dataset, and the second group included the remaining data (43 floods and 43 unfloods), which was used as the validation dataset (Shafizadeh-Moghadam et al., 2018; Choubin et al., 2019; Costache, 2019; Janizadeh et al., 2019; Khosravi et al., 2019; Tehrany et al., 2019).

### 3.2. 3.1. Flood influencing factors

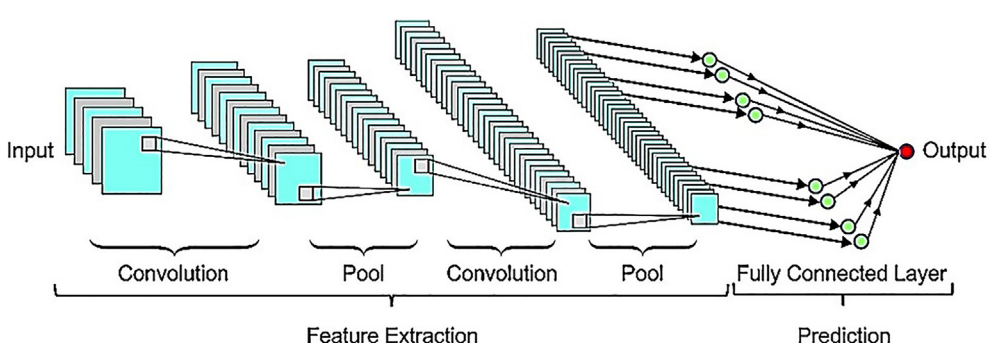
A prospective flood modeling requires exploring the spatial relationships between historical flood events and different geo-environmental variables that thought to directly or indirectly modulate the probability

**Table 1**  
Parameter settings for the CNN and RNN models.

Model	Parameter	Search space	Final settings
CNN	Convolutional kernel size	None	$3 \times 1$
	Number of convolution unit	30	30
	Max pooling kernel size	$3 \times 1$	$3 \times 1$
	Number of epochs	500	500
	Activation function	ReLU	ReLU
	Optimizer	Adamax	Adamax
	Learning rate	0.001	0.001
	Dropout rate	0.25	0.25
	Number of recurrent units	None	40
RNN	Number of epochs	40	500
	Activation function	ReLU	ReLU
	Optimizer	RMSprop	RMSprop
	Learning rate	0.001	0.001
	Dropout rate	0.2	0.2

of a flooding event. To select the most influential factors, we first considered a set of potential factors based on the flood modeling literature (Marco and Cayuela, 1994; Ouma and Tareishi, 2014; Nandi et al., 2016; Choubin et al., 2019; Janizadeh et al., 2019; Khosravi et al., 2019; Tehrany et al., 2019; Vojtek and Vojteková, 2019). We next reconsidered the initial set and selected the final set of influencing factors based on the local characteristics of the study area. Finally, we ended up with nine factors: slope degree, aspect, altitude, plan curvature, topographic wetness index (TWI), proximity to rivers, rainfall, land use, and lithology (Fig. 4).

Topographic features (slope, aspect, altitude, plan curvature, and TWI) have been repeatedly used as the main influencing factors for flood modeling because floods are strongly correlated with the topography. In general, floods tend to occur in flat and low-elevated areas (Janizadeh et al., 2019). Aspect and plan curvature are directly related to the convergence and direction of water flow, which control the probability of flood occurrences (Choubin et al., 2019; Darabi et al., 2019). TWI is a secondary factor derived from DEM that describes the hydrological settings of an area. Higher TWI values often point to areas with a high probability of flooding. We used a 30 m resolution ASTER Digital Elevation Model (DEM) obtained from the Alaska Satellite Facility (<https://vertex.daac.asf.alaska.edu>) to derive the maps of topographic features used in this study (Fig. 4a-d). Proximity to rivers is a crucial flood influencing factors due to the dependency of flooding to the terrestrial water storages (Jaafari et al., 2015b; Janizadeh et al., 2019). The map of proximity to rivers was generated using the Euclidian distance command in ArcGIS 10.3 (Fig. 4f). Rainfall is an important, and perhaps the most important, factor for the prediction of flash flood probability. Here, thirty years (1988–2018) metrological data from nine stations across the study area were interpolated using the simple kriging method to produce an annual rainfall map for the study area (Fig. 4g). Land-use type is often used as a proxy of human activities for explaining landscape modification and changing the land cover,

**Fig. 7.** Overall architecture of a CNN.

drainage system, and runoff hydrograph that usually result in flooding (Zope et al., 2016; Zhao et al., 2019a). The land-use map of the study area was produced from the Landsat 8 OLI satellite images using the maximum likelihood classification method that exhibited five land-use types across the study area (Fig. 4h). Finally, we included lithology into the modeling process because this factor characterizes soil and

underlying rock types and affects the infiltration and runoff in a catchment (Janizadeh et al., 2019; Zhao et al., 2019b). The lithology map of the study area was obtained from the National Cartographic Centre and Geological Survey of Iran (Fig. 4i). All calculations and generations of influencing factors were performed in ArcGIS 10.3 for a 30 m × 30 m pixel size.

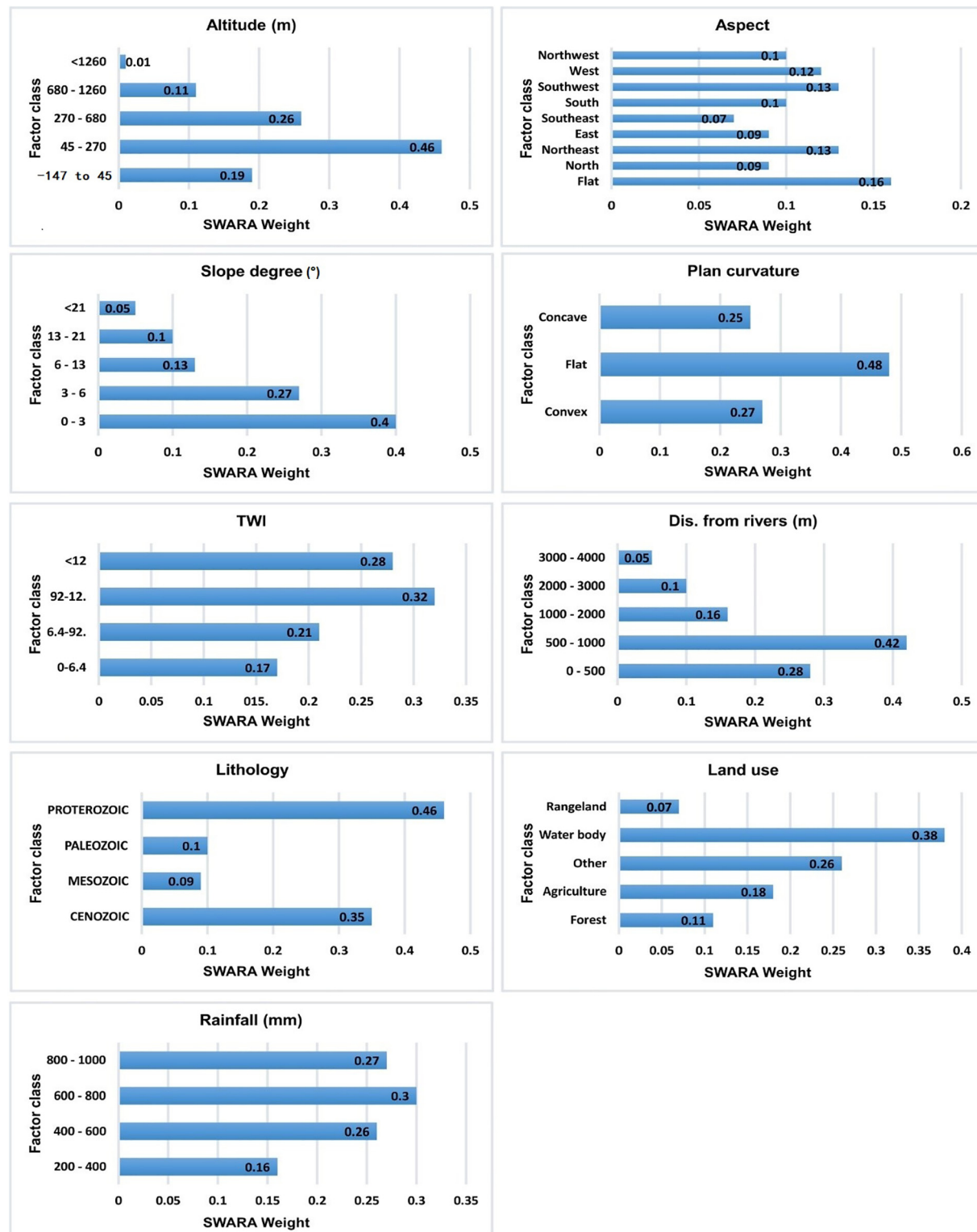


**Fig. 8.** Spatial relationship between each class of the influencing factors and floods extracted using the SWARA method.

## 4. Methodology

The flowchart of the methodology proposed in this study is shown in Fig. 5 and described as follows.

### 4.1. Factor importance

To investigate the spatial interplay between floods and different influencing factors toward quantifying the importance of each factor class, we used the step-wise weight assessment ratio analysis (SWARA) procedure (Keršulienė et al., 2010). SWARA is one of the most vastly used methods for calculating factor weight (Zolfani and Chatterjee, 2019), which performs under more straightforward computational process than the other multi-criteria decision-making techniques such as the analytic hierarchy process (AHP) and analytic network process (ANP) (Jaafari et al., 2015a, 2019a;). For estimating the importance of each factor class using the SWARA method, the classes of a given factor were prioritized based on their significance on flooding and the characteristics of the study area. Then, the classes were assigned a weight such that the highest weight was given to the most important class and the lowest weight was given to the least effective class. Finally, the overall rank of each class was obtained by averaging the expert rankings (Jaafari et al., 2019c). Using this procedure, each class of each flood influencing factor was assigned a weight that indicates the magnitude of the spatial association between each factor class and the probability of flooding.

### 4.2. Probability modeling

#### 4.2.1. Overview of deep learning architectures

Here, we only provide a brief description of the RNN and CNN architectures for assuring the completeness of the document. We refer the reader to the literature (LeCun et al., 1998; LeCun et al., 2015; Lipton et al., 2015; Kim, 2017; Kwon et al., 2017; Mahdavifar and Ghorbani, 2019) for a full description of the topic of deep learning and its different architectures.

RNN is the most common unsupervised (i.e., generative) deep learning architecture that can automatically learn from unlabeled raw data to deal with different classification problems. Structurally, RNN is inspired by the feed-forward neural network (FFNN) to enhance the capability for learning sequential data over several time steps. In traditional FFNN, the output of each unit is determined by the current input and is independent of the previous output of the same unit. Although this architecture is suited well for some applications, the architecture does not meet the context of some other real-world problems that use large sets of sequential data in which each sample depends upon the analysis of previous samples. In contrast to FFNN that just learns during the training, RNN can remember the patterns learned from prior inputs and decide based on the past and present conditions (Fig. 6). This ability allows for simultaneously modeling sequential and time dependencies on different scales.

CNN is another architecture of the deep learning that belongs to the family of supervised (i.e., discriminative) architectures. CNN is originated from the multilayer perceptron ANN and has established an important role in solving many prediction tasks problems, given its advantages compared to the models from traditional machine learning techniques (Mahdavifar and Ghorbani, 2019). Traditional ANNs represent a complex structure, in which each neuron in a hidden layer is totally linked to all neurons in the former layer. This fully-connected structure often fails to

**Table 2**

Training performance of the CNN and RNN models.

Metric	Model	
	CNN	RNN
Sensitivity (%)	85.53	83.55
Specificity (%)	82.89	80.26
Accuracy (%)	81.45	80.77
Kappa	0.795	0.788

**Table 3**

Validation performance of the CNN and RNN models.

Metric	Model	
	CNN	RNN
Sensitivity (%)	80.26	79.11
Specificity (%)	87.5	82.89
Accuracy (%)	78.19	77.85
Kappa	0.771	0.759

properly handle a large set of input data. To cope with this problem, CNN represents a hidden layer that consists of one or more convolutional layers, pooling layers, and fully connected layers (Fig. 7). Convolutional layers include several filters that split the input data into smaller dimensional parts. Pooling layers reduce the number of feature maps and make them robust against bias and noise. The fully connected layer combines all neurons to all neurons in the previous layer in order to integrate the data with group differentiation in the convolutional and pooling layers.

#### 4.2.2. Modeling procedure

The CNN and RNN deep learning neural networks were coded in the MATLAB programming language on a personal computer with a 3.30 GHz Intel(R) Core(TM) i5-4200u CPU, 4 GB of RAM, a x64-based processor, and the Microsoft Windows 8.1 operating system. Table 1 lists the parameter settings for the CNN and RNN deep learning models. After successful training and validation processes, the models were applied to the entire study area that was resulted in producing the probability indices ranging from 0 to 1. The indices were grouped and reclassified into five probability levels—very low, low, moderate, high, and very high—using the Natural Breaks (Jenks) classification method (Jenks and Caspall, 1971) available in ArcGIS. This procedure resulted in producing two distribution maps of flood probability occurrence for the study area.

### 4.3. Evaluation and comparison

Evaluation is a crucial step in probability modeling and without it, the outputs lack reliability. Various performance metrics have been used to evaluate the performance of the flood predictive models. In this study, we evaluated our models using the root-mean-square error (RMSE), sensitivity, specificity, precision, accuracy, F1 score, Kappa, and area under the receiver operating characteristic (ROC) curve (AUC) metrics. A detailed description on these metrics can be found in the literature (Pham et al., 2018; Bui et al., 2019b; Mafi-Gholami et al., 2019a, b; Moayedi et al., 2019b; Tran et al., 2020).

To statistically compare the performance of the CNN and RNN models, we used the Wilcoxon signed-rank test (WSRT). The application of WSRT was based on the probability indices obtained from the two phases of training and validation (Jaafari et al., 2019a). For each phase, the null hypothesis assumes that the indices are not statistically different at the significance level of  $p = 0.05$ . A critical  $z$ -value of  $-1.96 < z\text{-value} < 1.96$  indicates a  $p\text{-value} < 0.05$  and denies the null hypothesis, indicating that the differences are statistically significant (Hong et al., 2019).

## 5. Results and analysis

### 5.1. Spatial relationship

The spatial relationship between each class of the influencing factors and historical floods was measured using the SWARA method and revealed that the most flood-prone portions of the study area are located on flat curvature (SWARA<sub>weight</sub> = 0.48), PROTEROZOIC lithology unit (SWARA<sub>weight</sub> = 0.46), altitude of 45–270 m (SWARA<sub>weight</sub> = 0.46), distance from rivers of 500–1000 m (SWARA<sub>weight</sub> = 0.42) and slope degree of 0–3° (SWARA<sub>weight</sub> = 0.40). On the contrary, high-elevated (> 1260 m,

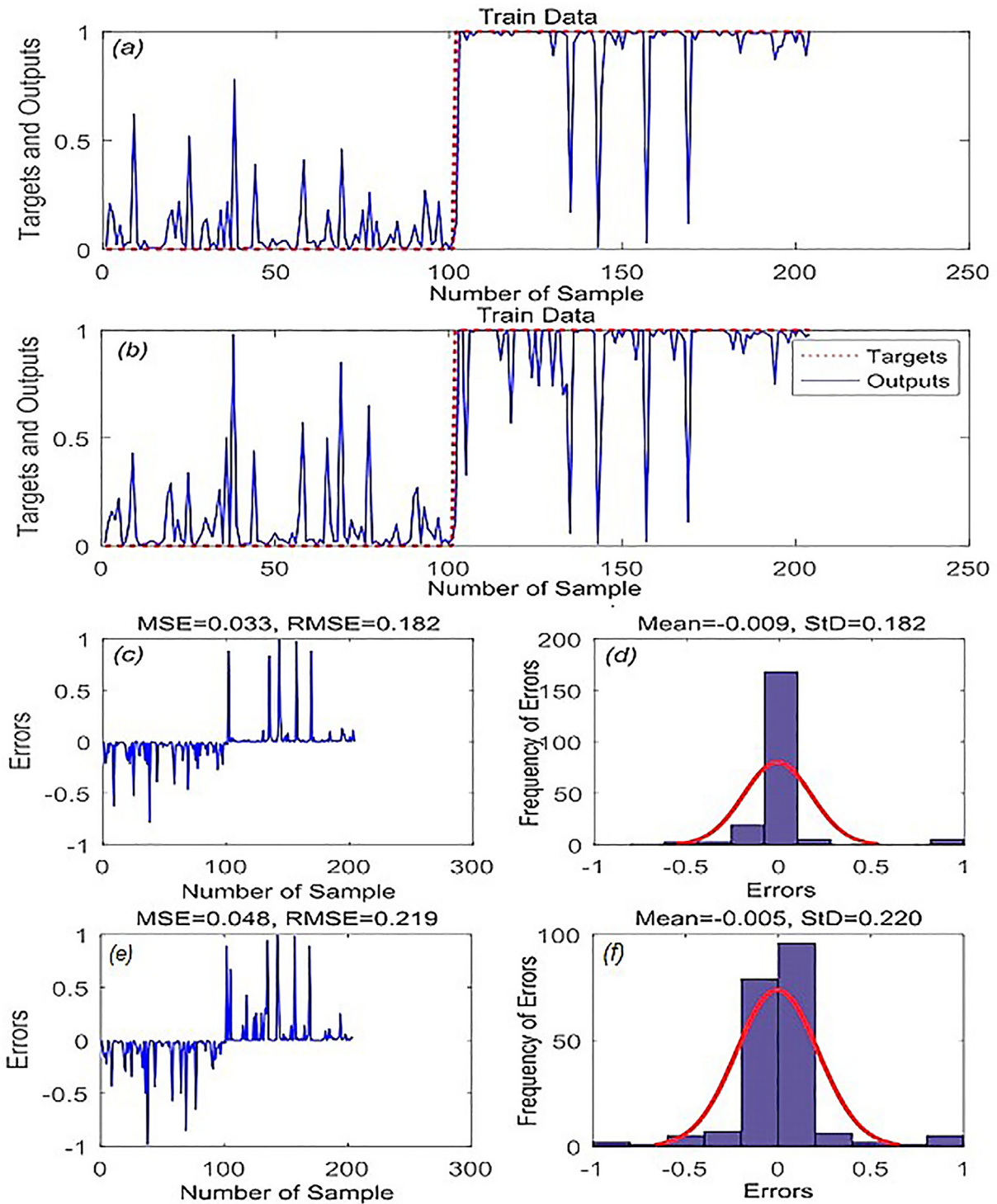


**Fig. 9.** Training performance of the models. (a) Magnitude of error for the CNN model; (b) magnitude of error for the RNN model; (c) RMSE of the CNN model; (d) error frequency for the CNN model; (e) RMSE of the RNN model; (f) error frequency for the RNN model.

SWARA<sub>weight</sub> = 0.01) and steep (slope degree > 21°, SWARA<sub>weight</sub> = 0.05) portions of the study area located in southeast aspects (SWARA<sub>weight</sub> = 0.06) and permit rangelands (SWARA<sub>weight</sub> = 0.07) were identified as the low-susceptible areas to flooding (Fig. 8).

## 5.2. Model performance

Training performance of the models (Table 2) showed that the CNN model with higher values of sensitivity (85.53%), specificity (82.89%), accuracy (81.45%), and Kappa (0.795) provided better goodness-of-fit with

the training dataset than the RNN model. In terms of the predictive ability, the CNN model achieved higher values of sensitivity (80.26%), specificity (87.5%), accuracy (78.19%), and Kappa (0.771) and successfully outperformed the RNN model and provided a more accurate estimate of future flooding (Table 3). Further, the CNN model with lower magnitude of training error provided better goodness-of-fit (RMSE = 0.182) and predictive ability (RMSE = 0.182) than the RNN model (Figs. 9 and 10).

The ROC method that computed the global performance of the models revealed that the two flood models used in this study with an AUC values of 0.86 (RNN) and 0.88 (CNN) have a reasonable

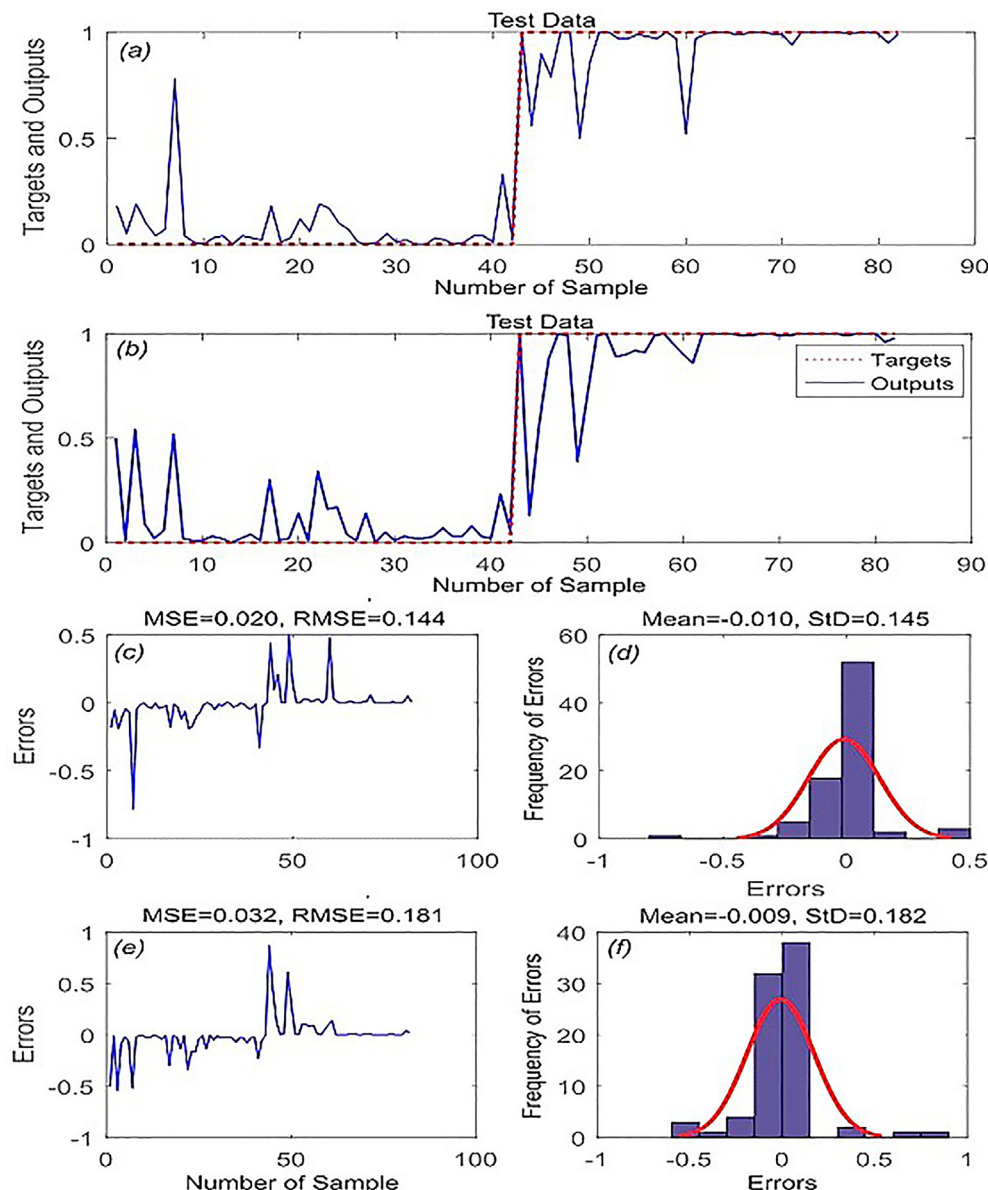


**Fig. 10.** Validation performance of the models. (a) Magnitude of error for the CNN model; (b) magnitude of error for the RNN model; (c) RMSE of the CNN model; (d) error frequency for the CNN model; (e) RMSE of the RNN model; (f) error frequency for the RNN model.

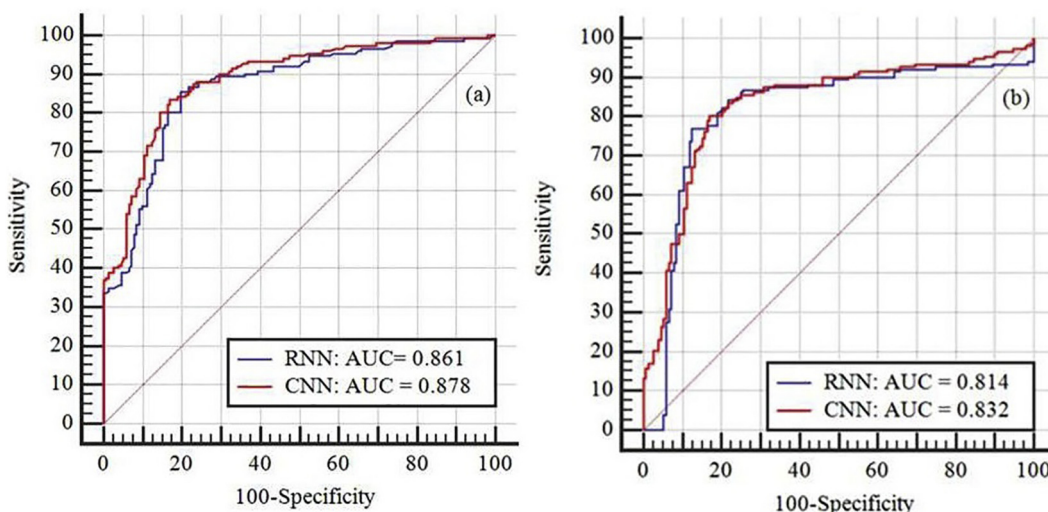


**Fig. 11.** AUC values of the RNN and CNN models in the training (a) and validation (b) phases.

goodness-of-fit with the training dataset (Fig. 11a). In the case of the validation dataset (i.e., ability to predict future floods), the results showed that the CNN model with an AUC value of 0.83 performed

marginally better than the RNN model (AUC = 0.81, Fig. 11b). Despite these differences, the results of the WSRT showed that these two deep learning models were not significantly different from each other either

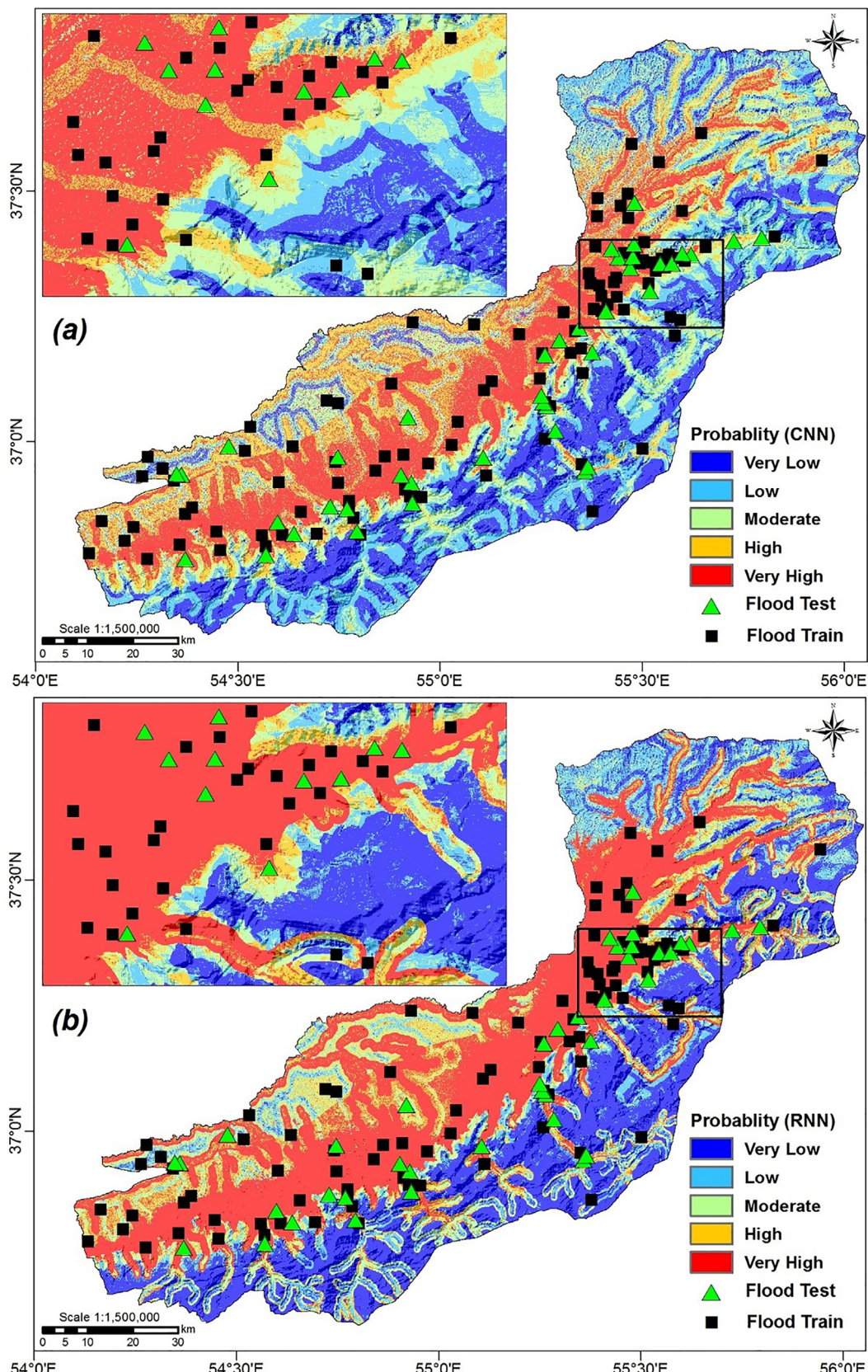


Fig. 12. Flood probability maps produced using the CNN (a) and RNN (b) models.

in the training phase ( $z$ -value = 0.634;  $p$ -value = 0.526) or in the validation phase ( $z$ -value = 0.365;  $p$ -value = 0.715).

### 5.3. Flood probability maps

The end products of the CNN and RNN models were two distribution maps that portray five levels of flood probability over the study region (Fig. 12). Quantitative analysis showed that approximately 20.5%, 20.2%, 20%, 23.6%, and 15.7% of the study area fall into very low, low, moderate, high, and very high probability of flood occurrence, respectively. Further analyses showed that in each map, the very high probability classes contain the greatest numbers of historical floods which are followed by the high, moderate, low, and very low classes, respectively, demonstrating that the models properly delimitated the study areas into different levels of probability to flood occurrence with respect to the historical events (Fig. 13).

## 6. Discussion

The SWARA technique identified the factor classes that contributed the most to flood occurrence in the study area. The first three classes

of altitude gained the greater SWARA weights than the other altitude classes that are in agreement with previous findings that demonstrated the frequent flooding in the low-elevated areas (Janizadeh et al., 2019). Given the virtually similar SWARA weights in the different classes of slope aspect, we can conclude that this factor does not significantly contribute to flooding in our study area. Despite the significant association between slope aspect and several landscape-level variables such as morphologic structures, amount of rainfall, vegetation distribution, and land-use type (Jaafari et al., 2017; Nami et al., 2018), the SWARA procedure failed to demonstrate a strong association between this factor and the floods that have occurred in the Golestan Province. Similar results have also been reported from the Hengfeng County of China (Hong et al., 2018), Brisbane catchment of Australia (Tehrany et al., 2019), Khiyav-Chai (Choubin et al., 2019) and Tafresh (Janizadeh et al., 2019) catchments of Iran, and Prahova river catchment of Romania (Costache, 2019). The low probabilities of flood occurrence were identified in the steep terrains (slope degree  $>6^\circ$ ) because these areas quickly convey the incoming rainfall to gentle slope areas and flat curvatures, where are more susceptible to flooding. Further, floods were more probable at a distance of 500–1000 m a river. The reduction of the flood probability on areas at a distance 0–500 m can be attributed

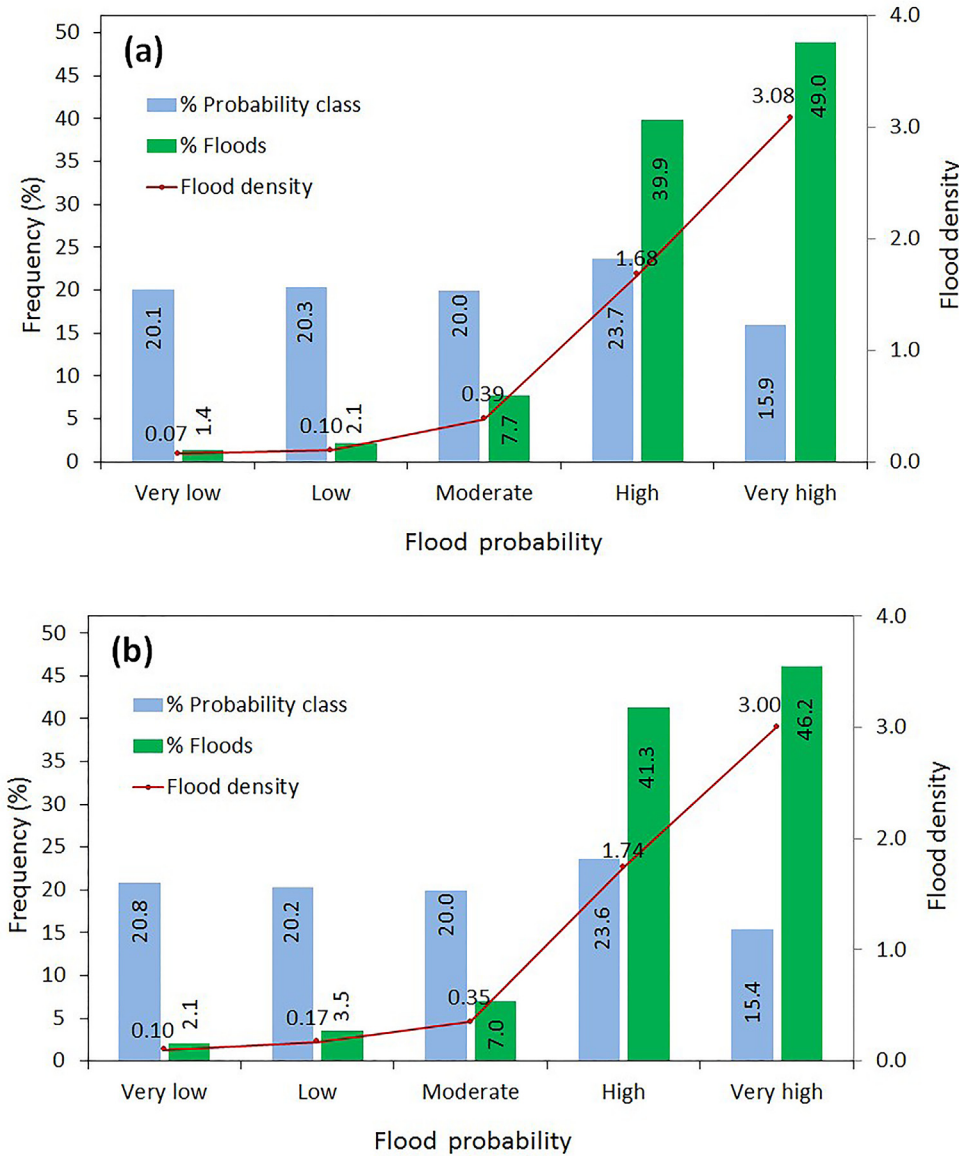


**Fig. 13.** Quantitative analysis of the flood probability maps derived by the (a) CNN and (b) RNN models.

to their altitude ( $> 700$  m), which had a negative association with flooding (Janizadeh et al., 2019). Overall, the low-elevated and gentle slope portions of the Golestan Province that permit the Cenozoic lithology unit and are mostly characterized by extensive human activities (e.g., farmlands and orchards) and received rainfall of 400–800 mm showed a strong association with flood occurrences. These portions of the province that cover ~40% of the land area and fall into high and very high levels of flood probability need to be supported by flood mitigation strategies and provided with the early warning systems.

In terms of the modeling approach, our results demonstrated that the deep learning modeling successfully improved flood prediction accuracy by ~17% compared to the most recent attempt by Ahmadlou et al. (2019), who used the same dataset and applied an adaptive neuro-fuzzy inference system (ANFIS) optimized by the biogeography-based optimization (BBO) and bat algorithm (BA) for flood prediction in the Golestan Province. These models yielded the prediction rates of 0.70 compared to our prediction rates of 0.814 (RNN) and 0.832 (CNN).

Our study area was a heterogeneous landscape characterized by diverse interacting environments, ranging from relatively natural territories, including forests and rangelands to human-dominated patches such as farmlands and settlements areas. To model and explore the information from such a landscape, we elected to use comparatively advanced models than those previously used by Ahmadlou et al. (2019). Our results suggest that the deep learnings are dominant over the models from traditional machine learning methods, which are line with those reported by Bui et al. (2019a), Gebrehiwot et al. (2019), and Sameen et al. (2019).

Accurate flood prediction generally requires analyzing a broad set of temporal and spatial data. Deep learning algorithms are more suitable for dealing with these datasets compared to SVM, ANN, neuro-fuzzy models (Ahmadlou et al., 2019; Bui et al., 2019a; Gebrehiwot et al., 2019; Sameen et al., 2019), whose performance is much dependent on the size of the dataset. This is also a sign of why SVM and neuro-fuzzy models are less accurate than CNN and RNN. SVM and neuro-fuzzy are comparable to a one-hidden layer of deep learning neural networks, which are obviously not capable enough to capture manifold environmental variables (Sameen et al., 2019; Wu et al., 2019). In addition, a modeling procedure based on the deep learning not only offers competitive performance for large datasets, but the automatic factor selection will also make this method more attractive, as modelers do not need to an optimized set of influencing factors (Janizadeh et al., 2019).

Although we have demonstrated an improved flood prediction using current models, there are still rooms for improvement that need to be considered in future works. For example, hyper-parameter tuning would certainly benefit the performance of the models and decrease the parameter uncertainty of the modeling. There are several hyper-parameters, such as network architecture, initialization, and activation method, that need to be properly tuned for the best performance. An attractive alternative for the traditional, time-consuming trial-and-error procedure is the integration of the deep learning neural networks with the metaheuristics optimization algorithms (e.g., genetic algorithms, particle swarm optimization, firefly algorithm, etc.) (Chen et al., 2019b; Jaadari et al., 2019a, b; Moayedi et al., 2019; Nguyen et al., 2019; Xi et al., 2019; Yuan and Moayedi, 2019) toward developing intelligent predictive models. Another research priority is the investigation of the effect of data size on model performance, as known, deep learning neural networks perform better particularly on large datasets (Wu et al., 2019). With the increase in the number of historic floods, we expect our models are capable of more accurately generalizing from the historical floods and recognizing underlying patterns of floods to predict future events (Jaafari et al., 2019a).

## 7. Conclusion

Flood probability mapping refers to the ability of managers, planners, and modelers to collect and analyze data from a variety of sources

to improve the understanding of factors affecting flooding and its spatial distribution. Here, we derived two advanced predictive models from the CNN and RNN deep learning algorithms for spatial prediction of floods in the Golestan Province, Iran. Using these models, the probability maps were generated at a fraction of the cost of manual probability assessments in the Golestan Province. Overall, our study showed that the spatially explicit deep learning neural network models are successful in capturing the heterogeneity of spatial patterns of flood probability in the Golestan Province.

Our results clearly demonstrated that future mitigation strategies should be directed to nearly 40% of the land area characterized by high and very susceptibility to flooding. Given the reasonable predictive accuracy and resolution quality, these maps can further be a useful and profitable tool for authorities and urban planners, principally as a screening tool to guide future developments of infrastructures in the province.

The first phase of a flood management strategy (i.e., identification of areas that are prone to flooding) was addressed in this study. Future research should be devoted to the second phase that is the development of flood risk mitigation plans. These plans that outline the overall strategies for reducing flood risk by reducing the flood hazard can include the modification of river systems, reduction of community vulnerability by moving people and their assets from the path of flood waters, and definition of the respective responsibilities for pre-flood planning, response and post-flood recovery.

The insights provided from this study help investigate other deep learning neural networks (e.g., generative models and auto encoders) for the prediction of flood probability. Future research may also seek to optimize the configuration of the CNN and RNN algorithms, since they still require extensive hyper-parameter tuning for the best performance.

## Declaration of competing interest

The authors declare that they have no known competing financial interests or personal relationships that could have appeared to influence the work reported in this paper.

## Acknowledgments

This research was conducted by the Basic Research Project of the Korea Institute of Geoscience and Mineral Resources (KIGAM) funded by the Ministry of Science and ICT.

## References

- Ahmadolou, M., Karimi, M., Alizadeh, S., Shirzadi, A., Parvinnejahad, D., Shahabi, H., Panahi, M., 2019. Flood susceptibility assessment using integration of adaptive network-based fuzzy inference system (ANFIS) and biogeography-based optimization (BBO) and bat algorithms (BA). *Geochem. Int.* 34 (11), 1252–1272.
- Alizadeh, M., Alizadeh, E., Asadollahpour Kotenaei, S., Shahabi, H., Beiranvand Pour, A., Panahi, M., Bin Ahmad, B., Saro, L., 2018. Social vulnerability assessment using artificial neural network (ANN) model for earthquake hazard in Tabriz city, Iran. *Sustainability* 10 (10), 3376.
- Azareh, A., Rahmati, O., Rafiei-Sardooi, E., Sankey, J.B., Lee, S., Shahabi, H., Ahmad, B.B., 2019. Modelling gully-erosion susceptibility in a semi-arid region, Iran: Investigation of applicability of certainty factor and maximum entropy models. *Sci. Total Environ.* 655, 684–696.
- Bayat, M., Ghorbanpour, M., Zare, R., Jaafari, A., Thai Pham, B., 2019. Application of artificial neural networks for predicting tree survival and mortality in the Hircanian forest of Iran. *Comput. Electron. Agric.* 164, 104929.
- Bui, D.T., Panahi, M., Shahabi, H., Singh, V.P., Shirzadi, A., Chapi, K., Khosravi, K., Chen, W., Panahi, S., Li, S., 2018a. Novel hybrid evolutionary algorithms for spatial prediction of floods. *Sci. Rep.* 8 (1), 15364.
- Bui, D.T., Shahabi, H., Shirzadi, A., Chapi, K., Pradhan, B., Chen, W., Khosravi, K., Panahi, M., Ahmad, B.B., Saro, L., 2018b. Land subsidence susceptibility mapping in South Korea using machine learning algorithms. *Sensors*. 18 (8), 2464.
- Bui, D.T., Hoang, N.-D., Martínez-Álvarez, F., Ngo, P.-T.T., Hoa, P.V., Pham, T.D., Samui, P., Costache, R., 2019a. A novel deep learning neural network approach for predicting flash flood susceptibility: a case study at a high frequency tropical storm area. *Sci. Total Environ.* 701, 134413.

- Bui, D.T., Moayedi, H., Gör, M., Jaafari, A., Foong, L.K., 2019b. Predicting slope stability failure through machine learning paradigms. *ISPRS Int. J. Geo-Inform.* 8 (9), 395.
- Bui, D.T., Ngo, P.-T.T., Pham, T.D., Jaafari, A., Minh, N.Q., Hoa, P.V., Samui, P., 2019c. A novel hybrid approach based on a swarm intelligence optimized extreme learning machine for flash flood susceptibility mapping. *Catena* 179, 184–196.
- Chen, W., Hong, H., Panahi, M., Shahabi, H., Wang, Y., Shirzadi, A., Pirasteh, S., Alesheikh, A.A., Khosravi, K., Panahi, S., 2019a. Spatial prediction of landslide susceptibility using GIS-based data mining techniques of ANFIS with whale optimization algorithm (WOA) and grey wolf optimizer (GWO). *Appl. Sci.* 9 (18), 3755.
- Chen, W., Panahi, M., Tsangaratos, P., Shahabi, H., Ilia, I., Panahi, S., Li, S., Jaafari, A., Ahmad, B.B., 2019b. Applying population-based evolutionary algorithms and a neuro-fuzzy system for modeling landslide susceptibility. *Catena* 172, 212–231.
- Choubin, B., Moradi, E., Golshan, M., Adamowski, J., Sajedi-Hosseini, F., Mosavi, A., 2019. An ensemble prediction of flood susceptibility using multivariate discriminant analysis, classification and regression trees, and support vector machines. *Sci. Total Environ.* 651, 2087–2096.
- Convertino, M., Annis, A., Nardi, F., 2019. Information-theoretic portfolio decision model for optimal flood management. *Environ. Model Softw.* 119, 258–274.
- Costache, R., 2019. Flash-flood potential assessment in the upper and middle sector of Prajova river catchment (Romania): A comparative approach between four hybrid models. *Sci. Total Environ.* 659, 1115–1134.
- Dao, D.V., Jaafari, A., Bayat, M., Mafi-Gholami, D., Qi, C., Moayedi, H., Phong, T.V., Ly, H.-B., Le, T.-T., Trinh, P.T., Luu, C., Quoc, N.K., Thanh, B.N., Pham, B.T., 2020. A spatially explicit deep learning neural network model for the prediction of landslide susceptibility. *Catena* 188, 104451.
- Darabi, H., Choubin, B., Rahmati, O., Torabi Haghghi, A., Pradhan, B., Kløve, B., 2019. Urban flood risk mapping using the GARP and QUEST models: a comparative study of machine learning techniques. *J. Hydrol.* 569, 142–154.
- Gebrehiwot, A., Hashemi-Beni, L., Thompson, G., Kordjamshidi, P., Langan, T.E., 2019. Deep convolutional neural network for flood extent mapping using unmanned aerial vehicles data. *Sensors*. 19 (7), 1486.
- Haynes, K., Coates, L., Van Den Honert, R., Gissing, A., Bird, D., Dimer De Oliveira, F., D'Arcy, R., Smith, C., Radford, D., 2017. Exploring the circumstances surrounding flood fatalities in Australia—1900–2015 and the implications for policy and practice. *Environ. Sci. Pol. Int.* 76, 165–176.
- Hong, H., Panahi, M., Shirzadi, A., Ma, T., Liu, J., Zhu, A.-X., Chen, W., Koulias, I., Kazakis, N., 2018. Flood susceptibility assessment in Hengfeng area coupling adaptive neuro-fuzzy inference system with genetic algorithm and differential evolution. *Sci. Total Environ.* 621, 1124–1141.
- Hong, H., Jaafari, A., Zenner, E.K., 2019. Predicting spatial patterns of wildfire susceptibility in the Huichang county, China: an integrated model to analysis of landscape indicators. *Ecol. Indic.* 101, 878–891.
- IRIMO, 2019. Islamic Republic of Iran Meteorological Organization (IRIMO). 2019. [Http://irimo.ir/english/monthly&annual/r25Asp](http://irimo.ir/english/monthly&annual/r25Asp) (Last accessed on 17.02.2019).
- Jaafari, A., Najafi, A., Melón, M.G., 2015a. Decision-making for the selection of a best wood extraction method: an analytic network process approach. *Forest Pol. Econ.* 50, 200–209.
- Jaafari, A., Najafi, A., Rezaeian, J., Sattarian, A., 2015b. Modeling erosion and sediment delivery from unpaved roads in the north mountainous forest of Iran. *GEM – Int. J. Geomathematics*. 6 (2), 343–356.
- Jaafari, A., Gholami, D.M., Zenner, E.K., 2017. A Bayesian modeling of wildfire probability in the Zagros mountains. *Ecol. Inform.* 39, 32–44.
- Jaafari, A., Panahi, M., Pham, B.T., Shahabi, H., Bui, D.T., Rezaie, F., Lee, S., 2019a. Meta optimization of an adaptive neuro-fuzzy inference system with grey wolf optimizer and biogeography-based optimization algorithms for spatial prediction of landslide susceptibility. *Catena* 175, 430–445.
- Jaafari, A., Razavi Termeh, S.V., Bui, D.T., 2019b. Genetic and firefly metaheuristic algorithms for an optimized neuro-fuzzy prediction modeling of wildfire probability. *J. Environ. Manag.* 243, 358–369.
- Jaafari, A., Zenner, E.K., Panahi, M., Shahabi, H., 2019c. Hybrid artificial intelligence models based on a neuro-fuzzy system and metaheuristic optimization algorithms for spatial prediction of wildfire probability. *Agric. For. Meteorol.* 266, 198–207.
- Jamali, B., Bach, P.M., Deletic, A., 2020. Rainwater harvesting for urban flood management – an integrated modelling framework. *Water Res.* 171, 115372.
- Janizadeh, S., Avand, M., Jaafari, A., Phong, T.V., Bayat, M., Ahmadisharaf, E., Prakash, I., Pham, B.T., Lee, S., 2019. Prediction success of machine learning methods for flash flood susceptibility mapping in the Tafresh watershed, Iran. *Sustainability* 11 (19), 5426.
- Jenks, G.F., Caspall, F.C., 1971. Error on choroplethic maps: Definition, measurement, reduction. *Ann. Assoc. Am. Geogr.* 61 (2), 217–244.
- Keršulienė, V., Zavadskas, E.K., Turskis, Z., 2010. Selection of rational dispute resolution method by applying new step-wise weight assessment ratio analysis (SWARA). *J. Bus. Econ. Manag.* 11 (2), 243–258.
- Khosravi, K., Pham, B.T., Chapi, K., Shirzadi, A., Shahabi, H., Revhaug, I., Prakash, I., Bui, D.T., 2018. A comparative assessment of decision trees algorithms for flash flood susceptibility modeling at Haraz watershed, northern Iran. *Sci. Total Environ.* 627, 744–755.
- Khosravi, K., Shahabi, H., Pham, B.T., Adamowski, J., Shirzadi, A., Pradhan, B., Dou, J., Ly, H.B., Gröf, G., Ho, H.L., Hong, H., Chapi, K., Prakash, I., 2019. A comparative assessment of flood susceptibility modeling using multi-criteria decision-making analysis and machine learning methods. *J. Hydrol.* 573, 311–323.
- Kim, P., 2017. Deep learning. Matlab deep learning. Springer, pp. 103–120.
- Kraus, M., Feuerriegel, S., Oztekin, A., 2019. Deep learning in business analytics and operations research: Models, applications and managerial implications. *Eur. J. Oper. Res.* 281 (3), 628–641.
- Kwon, D., Kim, H., Kim, J., Suh, S.C., Kim, I., Kim, K.J., 2017. A survey of deep learning-based network anomaly detection. *Clust. Comput.* 1–13.
- Lecun, Y., Bottou, L., Bengio, Y., Haffner, P., 1998. Gradient-based learning applied to document recognition. *Proc. IEEE* 86 (11), 2278–2324.
- Lecun, Y., Bengio, Y., Hinton, G., 2015. Deep learning. *Nature* 521 (7553), 436.
- Lee, S., Oh, H.J., 2019. Landslide susceptibility prediction using evidential belief function, weight of evidence and artificial neural network models (Korean Journal of Remote Sensing). 35 (2), 299–316.
- Lipton, Z.C., Berkowitz, J., Elkan, C., 2015. A critical review of recurrent neural networks for sequence learning. *arXiv Preprint arXiv:1506.00019*.
- Mafi-Gholami, D., Zenner, E.K., Jaafari, A., Bakhtiari, H.R., Tien Bui, D., 2019a. Multi-hazards vulnerability assessment of southern coasts of Iran. *J. Environ. Manag.* 252, 109628.
- Mafi-Gholami, D., Zenner, E.K., Jaafari, A., Ward, R.D., 2019b. Modeling multi-decadal mangrove leaf area index in response to drought along the semi-arid southern coasts of Iran. *Sci. Total Environ.* 656, 1326–1336.
- Mahdavifar, S., Ghorbani, A.A., 2019. Application of deep learning to cybersecurity: a survey. *Neurocomputing* 347, 149–176.
- Marco, J.B., Cayuela, A., 1994. Urban flooding: the flood-planned city concept. In: Rossi, G., Harmancıoglu, N., Yevjevich, V. (Eds.), Coping with Floods. NATO ASI Series (Series E: Applied Sciences). 257. Springer, Dordrecht. [https://doi.org/10.1007/978-94-011-1098-3\\_43](https://doi.org/10.1007/978-94-011-1098-3_43).
- Moayedi, H., Mehrabi, M., Kalantar, B., Abdullahi Mu'azu, M., Rashid, A.S., Foong, L.K., Nguyen, H., 2019a. Novel hybrids of adaptive neuro-fuzzy inference system (ANFIS) with several metaheuristic algorithms for spatial susceptibility assessment of seismic-induced landslide. *Geomatics Nat. Hazards Risk* 10 (1), 1879–1911.
- Moayedi, H., Tien Bui, D., Gör, M., Pradhan, B., Jaafari, A., 2019b. The feasibility of three prediction techniques of the artificial neural network, adaptive neuro-fuzzy inference system, and hybrid particle swarm optimization for assessing the safety factor of cohesive slopes. *ISPRS Int. J. Geo-Inform.* 8 (9), 391.
- Nami, M.H., Jaafari, A., Fallah, M., Nabuini, S., 2018. Spatial prediction of wildfire probability in the Hyrcanian ecoregion using evidential belief function model and GIS. *Int. J. Environ. Sci. Technol.* 15 (2), 373–384.
- Nandi, A., Mandal, A., Wilson, M., Smith, D., 2016. Flood hazard mapping in Jamaica using principal component analysis and logistic regression. *Environ. Earth Sci.* 75 (6), 465.
- Nguyen, H., Mehrabi, M., Kalantar, B., Moayedi, H., Abdullahi, M.a.M., 2019. Potential of hybrid evolutionary approaches for assessment of geo-hazard landslide susceptibility mapping. *Geomatics Nat. Hazards Risk* 10 (1), 1667–1693.
- Nguyen, P.T., Ha, D.H., Avand, M., Jaafari, A., Nguyen, H.D., Al-Ansari, N., Phong, T.V., Sharma, R., Kumar, R., Le, H.V., Ho, L.S., Prakash, I., Pham, B.T., 2020a. Soft computing ensemble models based on logistic regression for groundwater potential mapping. *Appl. Sci.* 10 (7), 2469.
- Nguyen, P.T., Ha, D.H., Jaafari, A., Nguyen, H.D., Van Phong, T., Al-Ansari, N., Prakash, I., Le, H.V., Pham, B.T., 2020b. Groundwater potential mapping combining artificial neural network and real AdaBoost ensemble technique: the Daknong province case-study, Vietnam. *Int. J. Environ. Res. Public Health* 17 (7), 2473.
- Nhu, V.-H., Janizadeh, S., Avand, M., Chen, W., Farzin, M., Omidvar, E., Shirzadi, A., Shahabi, H., Clague, J.J., Jaafari, A., Mansoorpoor, F., Pham, B.T., Ahmad, B.B., Lee, S., 2020a. Gis-based gully erosion susceptibility mapping: a comparison of computational ensemble data mining models. *Appl. Sci.* 10 (6), 2039.
- Nhu, V.-H., Shirzadi, A., Shahabi, H., Chen, W., Clague, J.J., Geertsema, M., Jaafari, A., Avand, M., Miraki, S., Asl, D.T., 2020b. Shallow landslide susceptibility mapping by random forest base classifier and its ensembles in a semi-arid region of Iran. *Forests*. 11 (4), 421.
- Nhu, V.-H., Shirzadi, A., Shahabi, H., Singh, S.K., Al-Ansari, N., Clague, J.J., Jaafari, A., Chen, W., Miraki, S., Dou, J., Luu, C., Górska, K., Thai Pham, B., Nguyen, H.D., Ahmad, B.B., 2020c. Shallow landslide susceptibility mapping: a comparison between logistic model tree, logistic regression, naïve Bayes tree, artificial neural network, and support vector machine algorithms. *Int. J. Environ. Res. Public Health* 17 (8), 2749.
- Ouma, Y., Tateishi, R., 2014. Urban flood vulnerability and risk mapping using integrated multi-parametric AHP and GIS: Methodological overview and case study assessment. *Water* 6 (6), 1515–1545.
- Pham, B.T., Prakash, I., Jaafari, A., Bui, D.T., 2018. Spatial prediction of rainfall-induced landslides using aggregating one-dependence estimators classifier. *J. Indian Soc. Rem. Sens.* 46 (9), 1457–1470.
- Pham, B.T., Jaafari, A., Prakash, I., Singh, S.K., Quoc, N.K., Bui, D.T., 2019. Hybrid computational intelligence models for groundwater potential mapping. *Catena* 182, 104101.
- Rahmati, O., Panahi, M., Kalantar, Z., Soltani, E., Falah, F., Dayal, K.S., Mohammadi, F., Deo, R.C., Tiefenbacher, J., Tien Bui, D., 2019. Capability and robustness of novel hybridized models used for drought hazard modeling in Southeast Queensland, Australia. *Sci. Total Environ.* 718, 134656.
- Sameen, M.I., Pradhan, B., Lee, S., 2019. Application of convolutional neural networks featuring Bayesian optimization for landslide susceptibility assessment. *Catena* 186, 104249.
- Sen, Z., 2018. Flood modeling, prediction and mitigation. Springer International Publishing.
- Shafizadeh-Moghaddam, H., Valavi, R., Shahabi, H., Chapi, K., Shirzadi, A., 2018. Novel forecasting approaches using combination of machine learning and statistical models for flood susceptibility mapping. *J. Environ. Manag.* 217, 1–11.
- Špitalar, M., Brilly, M., Kos, D., Žiberna, A., 2020. Analysis of flood fatalities–Slovenian illustration. *Water* 12 (1), 64.
- Tehrany, M.S., Pradhan, B., Mansor, S., Ahmad, N., 2015. Flood susceptibility assessment using gis-based support vector machine model with different kernel types. *Catena* 125, 91–101.
- Tehrany, M.S., Jones, S., Shabani, F., 2019. Identifying the essential flood conditioning factors for flood prone area mapping using machine learning techniques. *Catena* 175, 174–192.

- Tran, Q.C., Minh, D.D., Jaafari, A., Al-Ansari, N., Minh, D.D., Van, D.T., Prakash, I., 2020. Novel ensemble landslide predictive models based on the Hyperpipes Algorithm: a case study in the Nam Dam Commune, Vietnam. *App. Sci.* 10 (11), 3710.
- Vojtek, M., Vojteková, J., 2019. Flood susceptibility mapping on a national scale in Slovakia using the analytical hierarchy process. *Water* 11 (2), 364.
- Wu, L., Liu, Z., Bera, T., Ding, H., Langley, D.A., Jenkins-Barnes, A., Furlanello, C., Maggio, V., Tong, W., Xu, J., 2019. A deep learning model to recognize food contaminating beetle species based on elytra fragments. *Comput. Electron. Agric.* 166, 105002.
- Xi, W., Li, C., Moayedi, H., Nguyen, H., 2019. A particle-based optimization of artificial neural network for earthquake-induced landslide assessment in Ludian county, China. *Geomatics Nat. Hazards Risk* 10 (1), 1750–1771.
- Yuan, C., Moayedi, H., 2019. Evaluation and comparison of the advanced metaheuristic and conventional machine learning methods for the prediction of landslide occurrence. *Eng. Comput.* 1–11.
- Zhao, G., Pang, B., Xu, Z., Peng, D., Xu, L., 2019a. Assessment of urban flood susceptibility using semi-supervised machine learning model. *Sci. Total Environ.* 659, 940–949.
- Zhao, Y., Han, Q., Zhao, Y., Liu, J., 2019b. Soil pore identification with the adaptive fuzzy C-means method based on computed tomography images. *J. For. Res.* 30 (3), 1043–1052.
- Zolfani, S.H., Chatterjee, P., 2019. Comparative evaluation of sustainable design based on step-wise weight assessment ratio analysis (SWARA) and best worst method (BWM) methods: a perspective on household furnishing materials. *Symmetry* 11 (1), 74.
- Zope, P.E., Eldho, T.I., Jothiprakash, V., 2016. Impacts of land use–land cover change and urbanization on flooding: a case study of Oshiwara river basin in Mumbai, India. *Catena*. 145, 142–154.